Symmetry breaking of ionic semiconductors under pressure: the case of InAs

2009 J. Phys.: Condens. Matter 21 495801

(http://iopscience.iop.org/0953-8984/21/49/495801)

J. Phys.: Condens. Matter **21** (2009) 495801 (7pp) doi:10.1088/0953-8984/21/49/495801

Symmetry breaking of ionic semiconductors under pressure: the case of InAs

H Libotte[1], G Aquilanti[2], S Pascarelli[2], W A Crichton[2], T Le Bihan[2] and J P Gaspard[1]

[1] Condensed Matter Physics Laboratory, University of Liège, B5, B-4000 Sart-Tilman, Belgium
[2] European Synchrotron Radiation Facility, F-38043 Grenoble, France

Received 26 September 2009, in final form 26 October 2009
Published 13 November 2009
Online at stacks.iop.org/JPhysCM/21/495801

Abstract
The NaCl-to-*Cmcm* phase transition and the *Cmcm* structure of InAs under high pressure are studied by x-ray diffraction. The lattice parameters and fractional coordinates are given as a function of pressure. We propose a mechanism responsible for this type of symmetry breaking under pressure. We show that the ppσ interactions do not play a major role in the stabilization of the NaCl structure. Consequently the NaCl-to-*Cmcm* transition occurs only in compounds with a large charge transfer. General conclusions on the behavior of III–V semiconductors under pressure are drawn.

(Some figures in this article are in colour only in the electronic version)

1. Introduction

Under hydrostatic pressure, symmetry-lowering transitions have been observed in various materials such as group IV and III–V semiconductors [1, 2] and even in alkali metals [3–6]. The semiconductors show an open fourfold-coordinated structure at ambient pressure (diamond, zinc blende (ZB), würtzite). Earlier studies [7] have shown that the coordination number increases from 4 to 4 + 2 (β-Sn structure) for the more covalent compounds and from 4 to 6 (NaCl structure) for the more ionic compounds. Recently, it has been shown that the first or the second high-pressure phase can be less symmetrical than initially assumed. Indeed the systematics of the ionic III–V semiconductors under pressure has been reassessed [8, 9]. The existence of the β-Sn and NaCl structures for most III–V semiconductors has been shown to depend on the ionicity of the compound [10]. Moreover, the stability of the CsCl structure was also discussed in terms of dynamical instabilities [9].

The NaCl-to-*Cmcm* transition under pressure has been experimentally observed in several semiconductors [11, 12] in agreement with *ab initio* calculations [9, 13]. In this paper we focus on the high-pressure phase diagram of InAs, one of the most ionic III–V semiconductors [7]. The calculations of Mujica and Needs [13] have shown that the phase boundary between NaCl and *Cmcm* structures is difficult to locate. A study combining x-ray diffraction and x-ray absorption [2, 14, 15] showed that two distorted structures *Cmcm* and *Pmma* occur in the equilibrium phase diagram of InAs under pressure. The most recent observed structural sequence is thus ZB $\rightarrow$ NaCl $\rightarrow$ *Cmcm* $\rightarrow$ *Pmma* [2, 16].

The aim of this paper is twofold. First we determine the structural parameters of the high-pressure phases of InAs in the range (13–42) GPa, through refinement of angle-dispersive x-ray diffraction (ADXRD) data collected within a diamond anvil cell [2, 15]. Second, we propose a general mechanism of the symmetry lowering that occurs in III–V semiconductors under pressure, based on a semi-empirical quantum mechanical model. It is applied to the specific case of InAs. The role of the ionicity of the compound is also discussed.

This paper is organized as follows: in the first section we describe the *Cmcm* structure and the geometrical parameters used to describe the structural distortion process. Then we report the structural results of an ADXRD experiment at high pressure on InAs. In the next section a tight-binding model is described and the theoretical predictions are compared to the experimental results of ADXRD. The physical trends responsible for the behavior of InAs under pressure are finally discussed and several conclusions concerning the systematics of III–V semiconductors under pressure are drawn.

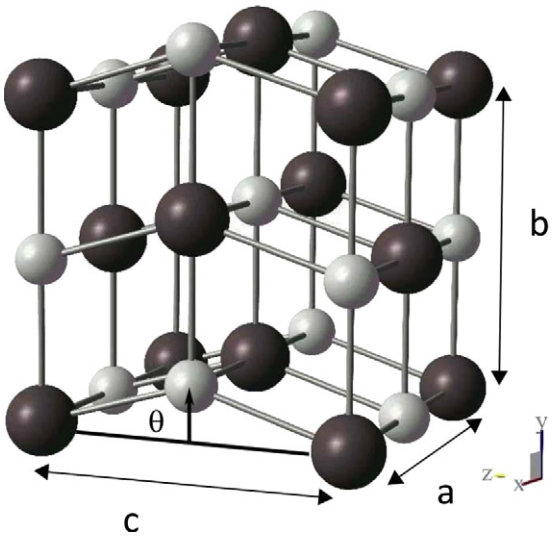

Figure 1. Idealized distorted NaCl structure used to model the *Cmcm* structure with the parameter θ.

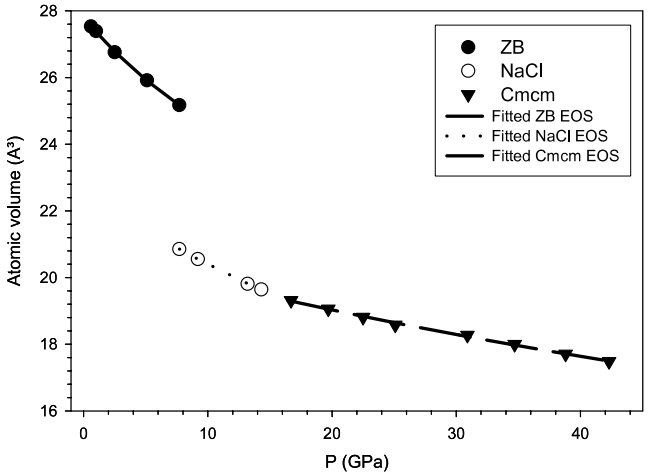

Figure 2. Relative atomic volume of InAs versus pressure for data recorded using nitrogen as pressure-transmitting medium. A change in atomic volume of ∼18% is associated with the ZB-to-NaCl transition. No volume discontinuity is observed during the NaCl-to-*Cmcm* phase transition.

2. Description of the *Cmcm* structure

The *Cmcm* structure is an orthorhombic distortion of the NaCl structure. In the orthorhombic cell with lattice parameters a, b and c, the In and As atoms are located on sites 4(c) of space group *Cmcm*, i.e. (0, y_1, $\frac{1}{4}$) and (0, y_2, $\frac{1}{4}$), respectively, with $y_2 - y_1 \cong \frac{1}{2}$. In the NaCl structure $y_1 = \frac{1}{4}$ and $y_2 = \frac{3}{4}$. The complete distortion can be considered as a triple symmetry breaking mechanism, with different components of decreasing amplitudes. The largest distortion is an alternating upwards and downwards shift of the (0 0 1) planes in the [0 1 0] direction (see figure 1). Zig-zag chains appear along the [0 0 1] direction; the distortion is characterized by the distortion angle θ given by $\tan\theta = \frac{2b}{c}(1 - y_1 - y_2) \cong \frac{b}{c}(1 - 4y_1)$. Typically θ is in the range (0°–20°). A second weaker orthorhombic distortion is also observed. The lattice parameters, a, b and c, remain, however, very close. The ratios of the lattice parameters depart from 1 by less than 10% ($c/b = 1.08$ at 42 GPa). Finally a third still smaller distortion (and still more negligible) occurs when $y_2 - y_1 \neq 0.5$. However, the relative departure of $y_2 - y_1$ from 0.5 is at the maximum 2%. It gives rise to four different interatomic distances that are shown in figure 5. We observe that, under the effect of pressure, the interatomic distance along the z axis, d_z, remains constant as well as the average interatomic distance along the y axis, $\frac{d_{y1}+d_{y2}}{2}$. In contrast, the interatomic distance along the x axis, d_x, decreases linearly with pressure.

We describe the *Cmcm* and NaCl structure in terms of two parameters a and θ as illustrated in figure 1. The NaCl structure is thus a special case of the *Cmcm* structure for $\theta = 0$. In the NaCl structure, the first six neighbors are at the same distance $\frac{a}{2}$. When only the angular distortion occurs, i.e. $\theta \neq 0$ with $y_2 - y_1 = \frac{1}{2}$, the six nearest neighbors split into two groups: four neighbors with an interatomic separation of $d_1 = \frac{a}{2}$ and two neighbors at $d_2 = \frac{a}{2\cos\theta}$.

3. Experimental results

ADXRD data on powdered InAs were recorded at the beamline ID30 of the European Synchrotron Radiation Facility (ESRF, Grenoble). The measurements have been performed using nitrogen as the pressure-transmitting medium. The experimental set-up is described in a previous paper [15] focusing on the observation of the phase transitions and on the description of the symmetry properties of the structures. In this paper, we present the results of a Rietveld refinement of the diffracted patterns giving the lattice parameters and atomic coordinates (see table 1). Moreover, the equations of state of the new phases are established.

Since the semi-empirical model described in the following sections is used to explain the NaCl-to-*Cmcm* distortion, the structural parameters presented here are relative to the structures of InAs up to the *Cmcm* phase. Figure 2 shows the relative volume per unit cell (normalized to the volume at room pressure) as a function of pressure.

In the ZB-to-NaCl phase transition we observe a huge volume discontinuity of ∼18%, consistent with a change in the coordination number, while no measurable volume discontinuity is associated with the NaCl-to-*Cmcm* phase transition. The experimental P–V points were fitted using the third-order Birch–Murnaghan equation of state (EoS). The relative parameters B_0, B_0' and $\frac{V}{V_0}|_{P=0}$ are reported in table 2.

The best refinements from 13.5 to 31 GPa result in an orthorhombic unit cell in space group *Cmcm*. Figures 3 and 4 show the structural parameters of InAs as a function of pressure. From 34 to 42 GPa we have fitted the data using a mixed *Cmcm* and *Pmma* phase. The *Pmma* parameters are not reported here. The deviation of y_1 and y_2 from $\frac{3}{4}$ and $\frac{1}{4}$ (values that correspond to the NaCl structure) is a further indication of the increase of the distortion of the *Cmcm* structure with respect to NaCl as a function of pressure. As illustrated in figure 4, the difference $y_1 - y_2$ remains very

Table 1. Structural parameters of InAs for zinc blende, NaCl and *Cmcm* structures measured by ADXRD.

Pressure (GPa)	a_{ZB} (Å)	a_{NaCl} (Å)	a_{Cmcm} (Å)	b_{Cmcm} (Å)	c_{Cmcm} (Å)	y_1	y_2
0.6	6.0395						
1.0	6.0292						
2.5	5.9821						
5.1	5.9186						
7.7	5.8616	5.5051					
9.2		5.4785					
13.2		5.4116					
14.3		5.3962					
16.7			5.3468	5.4088	5.3424	0.7064	0.2149
19.7			5.3143	5.4283	5.2849	0.6916	0.1951
22.5			5.2867	5.4365	5.2352	0.6836	0.1860
25.1			5.2625	5.4313	5.1996	0.6792	0.1797
30.9			5.2249	5.4252	5.1567	0.6714	0.1694
34.7			5.1938	5.4160	5.1184	0.6672	0.1633
38.8			5.1597	5.3987	5.0850	0.6651	0.1583
42.3			5.1307	5.3767	5.0700	0.6653	0.1551

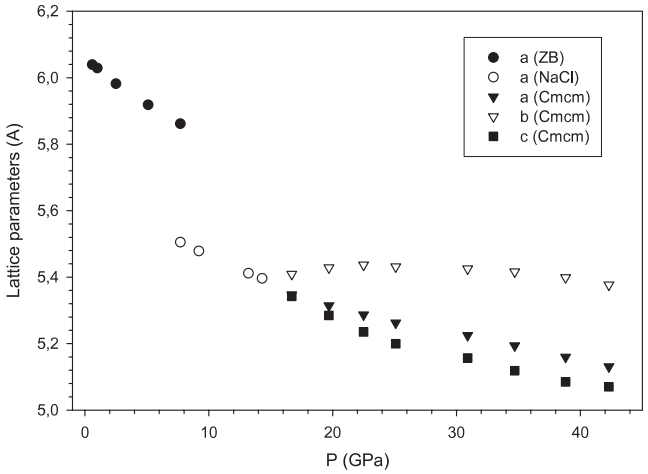

Figure 3. Experimental unit cell parameters versus pressure of ZB, NaCl and *Cmcm* structures of InAs.

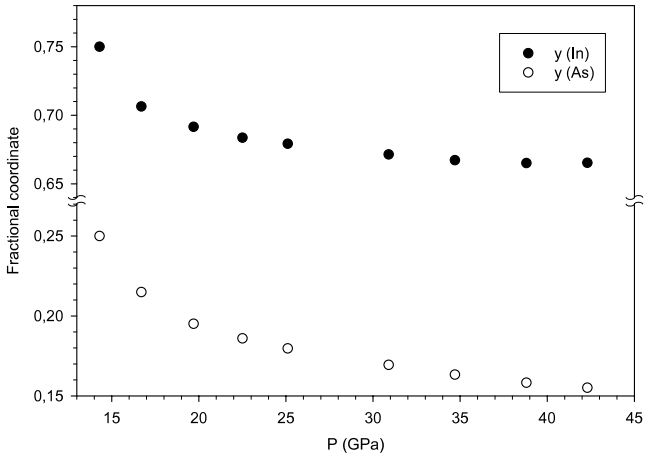

Figure 4. y values of In and As in the *Cmcm* structure as a function of pressure with $x = 0$ and $z = \frac{1}{4}$. The first point at 14.3 GPa corresponds to the NaCl structure.

Table 2. Structural parameters of InAs for ZB, NaCl and *Cmcm* structures using third-order Birch–Murnaghan equation of state.

Phase	B_0 (GPa)	B_0'	$\frac{V}{V_{0,ZB}}\|_{P=0}$
ZB	59.0 ± 2.0	5.3 ± 1.0	1.0
NaCl	65.7 ± 1.0	4.3 ± 1.0	0.825
Cmcm	191 ± 10	4.1 ± 1.0	0.750

close to 0.5; the relative departure from 0.5 is lower than 2%. The related distortion along the x axis is thus neglected in our theoretical description.

The InAs interatomic separations of the six nearest neighbors are depicted in figure 5. There are four different interatomic distances: the two distances in the x and z directions are identical but they are different distances y_1 and y_2 in the y direction. The average distances y_{av} are also depicted in figure 5. Two different behaviors appear: a strong linear variation of the x distances as a function of pressure and a fairly constant interatomic separation in the y and z directions. The behavior is highly anisotropic: inside the y–z plane the area is reduced by the zig-zag motion of the atoms as shown in figure 1, keeping the interatomic distances fairly constant. The θ angle clearly drives the decrease of the area.

4. Theoretical model

4.1. General considerations

The key point is the competition between the covalent and ionic contributions to the total energy. A simple model may account for the qualitative structural evolution of the III–V semiconductors under pressure. Let us assume that the total energy, E_{tot}, can be written as a sum of three contributions [17]: the band energy, the repulsive energy and the ionic energy. We have

$$E_{tot} = E_{cov} + E_{rep} + E_{ionic} = \int_{-\infty}^{E_F} E n_p(E)\,dE + \sum_{i<j} \frac{V_0}{r_{ij}^p} + E_{ionic} \quad (1)$$

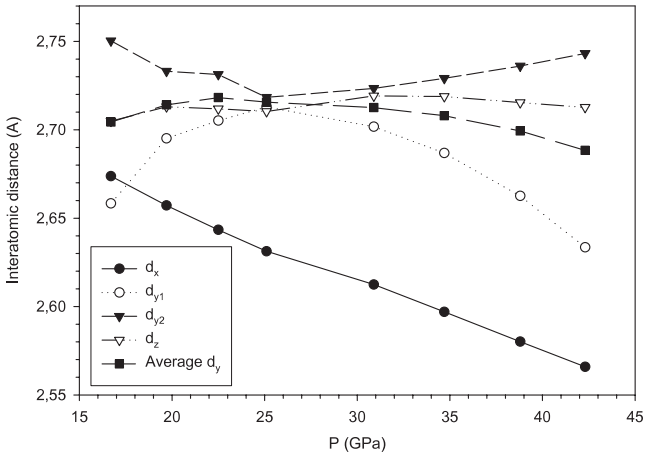

Figure 5. Interatomic separations in InAs as a function of pressure.

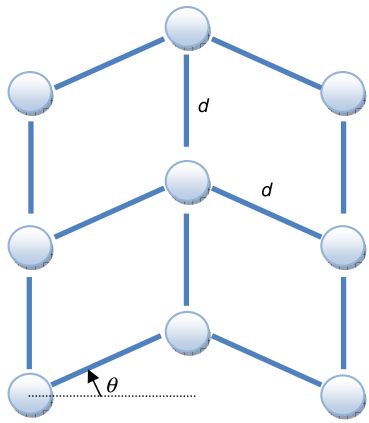

Figure 6. Simplified two-dimensional description of the deformed structure observed in the plane (1 0 0).

where

- $n_p(E)$ is the p-electron density of states filled up to the Fermi level E_F and r_{ij} are the distances between nearest-neighbor atoms i and j.
- The repulsive contribution is a classical pairwise additive potential between first neighbors only, with a strength V_0 and a hardness p. The higher the p value, the harder the repulsion.
- The Coulomb energy, E_{ionic}, depends on the structure in a complex way and on the atomic charges, $+Q$ and $-Q$, of In and As. So it has to be computed numerically. We used the GULP [22] software to evaluate the constant as a function of the distortion parameter, θ. We will first discuss the stability of the covalent system and therefore omit this term in the first step.

The stability of the structure under pressure requires us to evaluate the enthalpy, $H = E_{tot} + PV$.

In order to understand the physics of the NaCl-to-*Cmcm* distortion we first consider a 2D model that mimics the behavior in the (1 0 0) plane. We will focus on the angular rigidity of the structure and the pressure effects using two parameters, θ and d (figure 6). We assume that the interatomic distances d within the (1 0 0) plane remain constant in agreement with the experimental data. As we focus on the NaCl-to-*Cmcm* transition, the model has one free parameter, the distortion angle θ.

4.2. Covalent contribution

Let us consider a rhombohedral lattice in 2D. The unit cell parameters are $(2d\cos\theta, d)$ and the two distances are $r_1 = r_2 = d$ and the corresponding resonance integrals are equal $\beta_1 = \beta_2 = \beta$. The valence angles are $\pi/2 - \theta$ and $\pi/2 + \theta$.

In order to calculate E_{tot} for the high-pressure structures of InAs, i.e. NaCl and *Cmcm*, tight-binding calculations on a minimum basis including p orbitals only are enough to explain the distortion process (see section 5). Indeed the s electrons lie at lower energies and do not contribute significantly to the difference of cohesive energy as the related states are filled. In addition, as the valence angles are close to 90°, the s–p hybridization is negligible. The integral term in (1) involving the p-electron density of states, $n_p(E)$, is approximated by a three-peak distribution (the well-known Gauss quadrature technique). The positions of the three peaks and their strength are calculated via a moments technique [18–20]. Two shells of neighbors are considered, i.e. the moments of the density of states are calculated exactly up to the fourth moment μ_4 and the odd moments are zero. We use Kanamori's formula [23] to calculate the moments of the p-electron density of states including only ppσ couplings. The even moments of the density of states are easily calculated and the odd moments vanish because there are no odd membered rings of connected atoms. The covalent energy is calculated with only the ppσ interactions, the ppπ interactions being negligible[3]. The moment of order n is the sum of all the closed loops of length n, the internal angles of the loops are $\theta_1 \cdots \theta_n$:

$$\mu_n = (-1)^n \sum_{\text{loops of length } n} \beta_{pp\sigma_{0i}}(d_{0i})\beta_{pp\sigma_{ij}}(d_{ij}) \ldots \beta_{pp\sigma_{i0}}(d_{i0}) \times \cos\theta_1 \ldots \cos\theta_n \quad (2)$$

where $\beta_{pp\sigma,ij}$ are the σ resonance integrals between the p orbitals which are assumed to vary as an inverse power of the interatomic distance, d:

$$\beta_{pp\sigma}(d) = \frac{\beta_{pp\sigma,0}}{d^q} \quad (3)$$

where $\beta_{pp\sigma,0}$ and q are the physical parameters of the resonant interaction. For the sake of simplicity, the q value is chosen to be equal to 2 as suggested by Harrison [21].

At the transition pressure, we assume that the interatomic distances are all equal (to d) and so do the resonance integrals $\beta = \frac{\beta_{pp\sigma,0}}{d^q}$. The moments, normalized to unity, are given by

$$\mu_0 = 1$$
$$\mu_2 = 2\beta^2 \quad (4)$$
$$\mu_4 = 3\beta^4 + 2\beta^4\cos^2(2\theta) + 4\beta^4(2\sin^2\theta + \sin^4\theta)$$

The last terms in $\sin^4\theta$ correspond to non-self-retracing loops. The total of 36 closed loops corresponds to the fourth moment

[3] A discussion about this particular point is given in section 5.

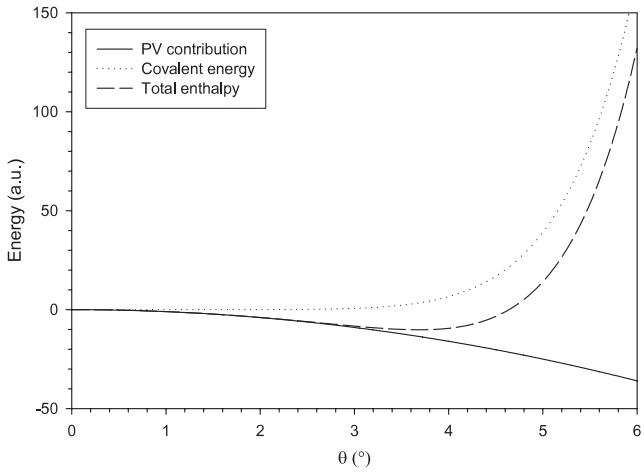

Figure 7. Simple description of the competition between enthalpic (PV) and covalent terms.

of the connectivity matrix. The series expansion in θ gives to the fourth order

$$\mu_4 \simeq 6\beta^4 + 12\beta^4\theta^4. \tag{5}$$

The coefficient of the θ^2 term is equal to zero and thus there is no restoring force in θ^2 due to the covalent ppσ interaction. The angular rigidity due to the ppσ is thus weak.

For an alternating system at the μ_4 level, as the odd moments vanish, the density of states $n_p(E)$ is represented by three levels at $-\sqrt{b_1+b_2}, 0, \sqrt{b_1+b_2}$ with the weights $\frac{b_1}{2(b_1+b_2)}, \frac{b_2}{b_1+b_2}, \frac{b_1}{2(b_1+b_2)}$, respectively. As the repulsive energy is independent of θ, the total energy can be discussed in terms of the electronic energy alone.

Let us assume that the distances remains equal, i.e. the μ_2 term is then constant and the lowest-order correction to μ_4 is in θ^4. If an extra term, angularly dependent, is added to the fourth-order moment, the fourth moment is $\mu_4 = \mu_4^0 + f(\theta)$. We have

$$b_1 = 2\beta^2 \qquad b_2 = b_2^0 + \frac{f}{2\beta^2}. \tag{6}$$

The three energy levels, E_1, E_2 and E_3, are at

$$E_1 = -\sqrt{3\beta^2 + \frac{f}{2\beta^2}} \simeq -\sqrt{3}\left(1 + \frac{f}{12\beta^4}\right) = -E_3 \tag{7}$$

$$E_2 = 0 \tag{8}$$

and the weights a_i:

$$a_1 = \frac{4\beta^4}{2(6\beta^4 + f)} \simeq \frac{1}{3}\left(1 - \frac{f}{6\beta^4}\right) = a_3 \tag{9}$$

$$a_2 = \frac{2\beta^4 + f}{6\beta^4 + f} \simeq \frac{1}{3}\left(1 + \frac{f}{3\beta^4}\right). \tag{10}$$

For a 1/3 filling of the p band, we show that the restoring force is weak. Indeed

(i) if f is positive, the energy level E_1 moves to more negative values but its weight is reduced (twice as much). Finally the total energy $E_{\rm cov} = \frac{\sqrt{3}}{3}\beta(1 - \frac{f}{12\beta^4})$ is less favorable than without distortion.

Table 3. Values of the electronic parameters obtained from the fit of the model to the experimental $V(P)$ curve for each structure in competition.

$\frac{p}{q}$	$\frac{V_0}{d^p_{0,ZB}}$ (eV)	$\frac{Q}{e}$
3.5	0.373	0.39

(ii) if f is negative, the weight a_1 gets larger than 1/3 and a_1 has to be limited to 1/3. The total energy $E_{\rm cov} = \frac{\sqrt{3}}{3}\beta(1 + \frac{f}{12\beta^4})$ is again less favorable than without distortion.

Finally

$$E_{\rm cov} = \frac{\sqrt{3}}{3}\beta\left(1 - \frac{|f|}{12\beta^4}\right) \simeq \frac{\sqrt{3}}{3}\beta(1 - \theta^4). \tag{11}$$

In conclusion, the distortion is unfavored, independently of the sign of f, i.e. the system is stable against an angular distortion for a 1/3 filling. This is true to the fourth order in the moments' expansion (three energy levels) and for a 1/3-filled p band. An exact calculation in 2D confirms this finding.

The parameters used in the tight-binding model (p/q, $V_0/d^p_{0,ZB}$, Q/e) are given in table 3.

At the fourth moment, the electronic density of states is approximated using three levels: $(-\sqrt{\frac{\mu_4}{\mu_2}}, 0, \sqrt{\frac{\mu_4}{\mu_2}})$. In our case with a $\frac{1}{3}$ band filling, only the filling of the first level is significant for the structural properties. The weight of this first level is $\frac{\mu_2^2}{\mu_4}$. The resulting attractive energy is simply

$$E_{\rm cov} = -\min\left(\frac{\mu_2^2}{\mu_4}, \frac{1}{3}\right)\sqrt{\frac{\mu_4}{\mu_2}}. \tag{12}$$

4.3. Enthalpic contribution

Pressure effects favor the distortion. Indeed the surface of the rhombus decreases (see figure 6) with θ and its series expansion has a negative θ^2 contribution. This term makes the distorted structure more stable. Figure 7 illustrates the competition between the covalent and enthalpic (PV) terms.

4.4. Electrostatic contribution

Up to now the electrostatic contribution was omitted. With the GULP software, the Madelung constant can be calculated as a function of the angle θ. A numerical fit of the Madelung constant to the fourth order in θ gives $\alpha_{\rm M} = 1.747\,58 - 0.7058\theta^2 + 6.962\theta^4$ with θ expressed in radians. An analytic calculation of the variation of the Madelung constant involving only the displacement of the atoms of the first coordination shell gives $\alpha_{\rm M} = 1.747\,58 - \sqrt{0.5}\theta^2$ up to the second order in θ, in excellent agreement with the numerical values. Thus, the ionic term is

$$E_{\rm ionic} = -(1.747\,58 - 0.7058\theta^2 + 6.962\theta^4)\frac{Q^2}{4\pi\epsilon_0}\frac{1}{d}. \tag{13}$$

The θ^4 term is one order of magnitude smaller than the θ^2 contribution.

In summary, let us stress that the ionic contribution is the sole contribution with a restoring force (energy) in the θ^2 term which stabilizes the undistorted NaCl structure.

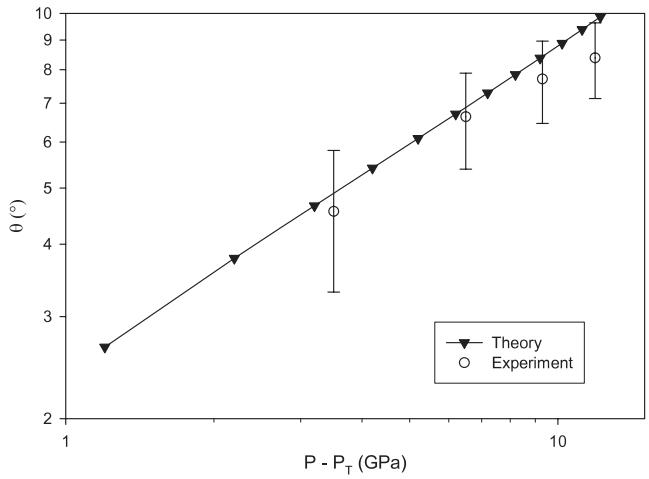

Figure 8. Comparison of the theoretical and experimental variations of the θ angle in the $Cmcm$ phase.

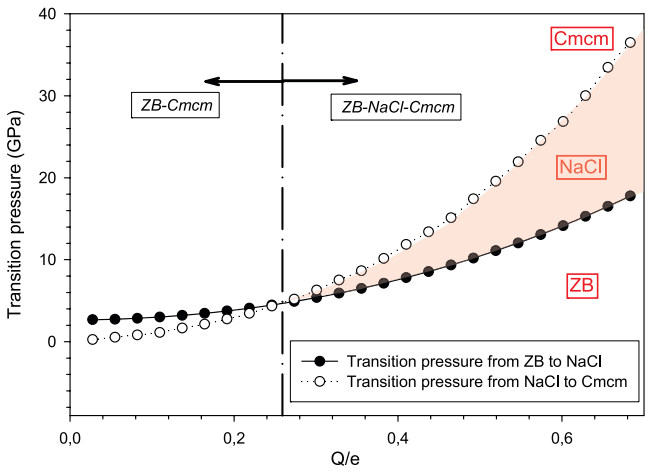

Figure 9. Evolution of the transition pressures as a function of the charge transfer, $\frac{Q}{e}$. ZB energy is calculated with the same model. The shaded area illustrates the stability range of the NaCl structure.

4.5. Total enthalpy

The parameters $(\beta_0, V_0, \frac{p}{q})$ are obtained by fitting the theoretical model to the experimental equation of states, i.e. the bulk modulus, B_0, its pressure derivative, B_0', and the zero-pressure lattice parameter, a_0, of the different phases, obtained from our ADXRD data and reported in table 2. The enthalpy of the NaCl and $Cmcm$ structures can be written at the fourth order in θ:

$$H = H_0 + \left(-\frac{1}{2}Pd_{0,\mathrm{NaCl}}^3 + 0.7058\frac{Q^2}{4\pi\epsilon_0}\right)\theta^2 + \left(\frac{1}{24}Pd_{0,\mathrm{NaCl}}^3 + 2.645\frac{\beta_{\mathrm{pp}\sigma}^0}{d_{0,\mathrm{NaCl}}^2} - 6.962\frac{Q^2}{4\pi\epsilon_0}\right)\theta^4 \quad (14)$$

where H_0 is the enthalpy calculated for $d = d_T$, the interatomic distance at the transition. Both $\beta_{\mathrm{pp}\sigma}^0$ and $\beta_{\mathrm{pp}\pi}^0$ are positive. $d_{0,\mathrm{NaCl}}$ is the interatomic distance in the NaCl structure at 0 GPa. The enthalpic contribution in the θ^4 coefficient is one order of magnitude smaller than the covalent contribution.

5. Discussion

Calculations of the band structure with ppπ interactions induces a θ^2 term. However, its intensity is one order of magnitude smaller than the electrostatic contribution.

Figure 8 shows the evolution of θ as a function of the pressure. The agreement between the experimental values and the model is correct up to 8 GPa above the transition pressure. At higher pressures, the increase of $\theta(P)$ of the theoretical model is faster than the experimental data because some contributions of the restoring force have been neglected (the effect of ppπ interactions, second-neighbor repulsion, etc).

The NaCl phase is stable when ionicity is high. Stabilization is tightly linked to the relative importance of the electrostatic contribution (Madelung term). Thus, when the electrostatic contribution is added to the enthalpy expression we now have a competition between the pressure and the electrostatic contribution, giving rise to a critical pressure, P_{cr}, as there is no θ^2 term arising from the covalent contribution. The expression for this critical pressure is

$$P_{\mathrm{cr}} = 0.3528\frac{Q^2}{\pi\epsilon_0 d_{0,\mathrm{NaCl}}^3} \quad (15)$$

Actually, the transition pressure is thus a direct image of the ionicity as illustrated in figure 9.

The NaCl-to-$Cmcm$ transition is a second-order transition calculated to occur at 12.5 GPa. The transition pressure is determined from the $E(V)$ curves of both phases. Figure 9 shows the evolution of the transition pressures from ZB-to-NaCl and from NaCl-to-$Cmcm$ as a function of the charge transfer, $\frac{Q}{e}$. The stability range of the NaCl increases with the charge transfer. As the ionic interaction is isotropic, it stabilizes the NaCl structure, more symmetrical than $Cmcm$. This is in agreement with experimental data related to other III–V semiconductors. InP and InAs, the more ionic semiconductors, exhibit NaCl structure in their phase diagrams whereas GaP and GaAs do not [10, 11, 14, 25–27] as summarized in table 4. Once the NaCl is present, pressure induces the NaCl-to-$Cmcm$ distortion.

6. Conclusion

In this paper we determine the structural parameters for the NaCl and $Cmcm$ phases of InAs up to 42 GPa. A general mechanism of symmetry lowering of highly symmetric (NaCl) structures is described and applied to III–V semiconductors. This description is based on a simple semi-empirical model that allows the identification of the physical parameters responsible for the distortion mechanism. The NaCl structure occurs only in highly ionic systems, as the stability range of the NaCl phase vanishes if the charge transfer is not high enough, as shown in figure 9. This explains the qualitative difference observed in the phase diagrams of III–V semiconductors. In the case of InAs, the ionicity is high enough to stabilize the NaCl phase on a limited pressure range, i.e. between 9.2 and 13.5 GPa. We analyze the different parameters that stabilize the

Table 4. Experimental data for GaAs, GaP, InAs and InP are compared with theoretical predictions.

Compound	Ionicity [24]	Crystallographic structures and related experimental transition pressures	Calculated transition pressures
InP	0.506	ZB $\xrightarrow[9.8\,\mathrm{GPa}]{}$ NaCl $\xrightarrow[28\,\mathrm{GPa}]{}$ *Cmcm*	ZB $\xrightarrow[10.5\,\mathrm{GPa}]{}$ NaCl $\xrightarrow[19.5\,\mathrm{GPa}]{}$ *Cmcm*
InAs	0.450	ZB $\xrightarrow[9.2\,\mathrm{GPa}]{}$ NaCl $\xrightarrow[13.5\,\mathrm{GPa}]{}$ *Cmcm*	ZB $\xrightarrow[7.8\,\mathrm{GPa}]{}$ NaCl $\xrightarrow[12.5\,\mathrm{GPa}]{}$ *Cmcm*
GaP	0.371	ZB $\xrightarrow[24\,\mathrm{GPa}]{}$ *Cmcm*	ZB $\xrightarrow[4\,\mathrm{GPa}]{}$ *Cmcm*
GaAs	0.316	ZB $\xrightarrow[17.3\,\mathrm{GPa}]{}$ *Cmcm*	ZB $\xrightarrow[3.8\,\mathrm{GPa}]{}$ *Cmcm*

NaCl structure. The ppσ interactions hardly stabilize the NaCl structure as the restoring force is not linear in the deformation angle θ but is proportional to θ^3 for small deformations. A restoring force in θ comes from the ionic term with an additional weaker ppπ interaction. In conclusion the angular stability of NaCl is marginal for ionocovalent systems, hence the rarity of the rocksalt structure.

Acknowledgments

The FNRS and the EU (NoE FAME) are gratefully acknowledged for their support.

References

[1] McMahon M I and Nelmes R J 1993 *Phys. Rev.* B **47** R8337
[2] Pascarelli S, Aquilanti G, Crichton W A, Le Bihan T, Mezouar M, De Panfilis S, Itié J P and Polian A 2003 *Europhys. Lett.* **61** 554
[3] Christensen N E and Novikov D L 2001 *Solid State Commun.* **119** 477
[4] Neaton J B and Ashcroft N W 1999 *Nature* **400** 141
[5] Schwarz U, Takemura K, Hanfland M and Syassen K 1998 *Phys. Rev. Lett.* **81** 2711
[6] Angilella G G N, Siringo F and Pucci R 2003 *Eur. Phys. J.* B **32** 323
[7] Phillips J C 1974 *Bonds and Bands in Semiconductors* (New York: Academic)
[8] Kim K, Ozoliņš V and Zunger A 1999 *Phys. Rev.* B **60** R8449
[9] Ozoliņš V and Zunger A 1999 *Phys. Rev. Lett.* **82** 767
[10] Nelmes R J and McMahon M I 1998 *Semiconductors and Semimetals* vol 54 (New York: Academic)
[11] Nelmes R J, McMahon M I and Belmonte S A 1997 *Phys. Rev. Lett.* **79** 3668
[12] Vohra Y K, Weir S T and Ruoff A L 1985 *Phys. Rev.* B **31** 7344
[13] Mujica A and Needs R J 1997 *Phys. Rev.* B **55** 9659
[14] Pascarelli S, Aquilanti G, Crichton W A, Le Bihan T, De Panfilis S, Fabiani E, Mezouar M, Itié J P and Polian A 2002 *High Press. Res.* **22** 331
[15] Aquilanti G, Crichton W A, Le Bihan T and Pascarelli S 2003 *Nucl. Instrum. Methods* B **200** 90
[16] Nelmes R J, McMahon M I, Wright N G, Allan D R, Liu H and Loveday J S 1995 *J. Phys. Chem. Solids* **56** 539
[17] Majewski J A and Vogl P 1987 *Phys. Rev.* B **35** 9666
[18] Gaspard J P and Cyrot-Lackmann F 1973 *J. Phys. C: Solid State Phys.* **6** 3077
[19] Haydock R, Heine V and Kelly M J 1975 *J. Phys. C: Solid State Phys.* **8** 2591
[20] Stoer J and Bulirsch R 1980 *Introduction to Numerical Analysis* (New York: Springer)
[21] Harrison W A 1980 *Electronic Structure and the Properties of Solids* (San Francisco: Freeman)
[22] Gale J D 1997 *J. Chem. Soc. Faraday Trans.* **93** 629
[23] Kanamori J 1966 *Progr. Theor. Phys.* **35** 16
[24] Garcia A and Cohen M L 1993 *Phys. Rev.* B **47** 4215
[25] Aquilanti G, Libotte H, Crichton W A, Pascarelli S, Trapananti A and Itié J-P 2007 *Phys. Rev.* B **76** 1
[26] Aquilanti G and Pascarelli S 2005 *J. Phys.: Condens. Matter* **17** 1811
[27] Smolentsev G, Soldatov A V, Pascarelli S and Aquilanti G 2006 *J. Phys.: Condens. Matter* **18** 7393